Technical Note: Single-shell δ¹¹B analysis of *Cibicidoides wuellerstorfi* using femtosecond laser ablation MC-ICPMS and secondary ion mass spectrometry

Markus Raitzsch[1,2,3], Claire Rollion-Bard[4], Ingo Horn[1], Grit Steinhoefel[2], Albert Benthien[2], Klaus-Uwe Richter[2], Matthieu Buisson[4], Pascale Louvat[4], Jelle Bijma[2]

[1]Institut für Mineralogie, Leibniz Universität Hannover, Callinstraße 3, 30167 Hannover, Germany
[2]Alfred-Wegener-Institut, Helmholtz-Zentrum für Polar- und Meeresforschung, Am Handelshafen 12, 27570 Bremerhaven, Germany
[3]MARUM - Zentrum für Marine Umweltwissenschaften, Universität Bremen, Leobener Straße 8, 28359 Bremen, Germany
[4]Université de Paris, Institut de physique du globe de Paris, CNRS, F-75005 Paris, France

Correspondence to: Markus Raitzsch (mraitzsch@marum.de)

Abstract. The boron isotopic composition (δ¹¹B) of benthic foraminifera provides a valuable tool to reconstruct past deep-water pH. As the abundance of monospecific species might be limited in sediments, microanalytical techniques can help to overcome this problem, but such studies on benthic foraminiferal δ¹¹B are sparse. In addition, microanalytics provide information on the distribution of δ¹¹B at high spatial resolution to increase the knowledge of e.g. biomineralization processes. For this study, we investigated the intra- and inter-shell δ¹¹B variability of the epibenthic species *Cibicidoides wuellerstorfi*, which is widely used in paleoceanography, by secondary ion mass spectrometry (SIMS) and femtosecond laser ablation multicollector inductively coupled plasma mass spectrometry (LA-MC-ICPMS). While the average δ¹¹B values obtained from these different techniques agree remarkably well with bulk solution values to within ±0.1 ‰, a relatively large intra-shell variability was observed. Based on multiple measurements within single shells, the SIMS and LA data suggest median variations of 4.8 ‰ and 1.3 ‰ (2σ), respectively, where the larger spread for SIMS is attributed to the smaller volume of calcite being analyzed in each run. When analytical uncertainties and volume-dependent differences in δ¹¹B variations are taken into account for these methods, the intra-shell variability is estimated to be in the order of ~3 ‰ and ~0.4 ‰ (2σ) on a ~20 μm and 100 μm scale, respectively. In comparison, the δ¹¹B variability between shells exhibits a total range of ~3 ‰ for both techniques, suggesting that several shells need to be analyzed for accurate mean δ¹¹B values. Based on a simple resampling method, we conclude that ~12 shells of *C. wuellerstorfi* must be analyzed using LA-MC-ICPMS to obtain an accurate average value within ±0.5 ‰ (2σ) to resolve pH variations of ~0.1. Based on our findings, we suggest to prefer the conventional bulk solution MC-ICPMS over the in-situ methods for e.g. paleo-pH studies. However, SIMS and LA provide powerful tools for high-resolution paleoreconstructions, or for investigating ontogenetic trends in δ¹¹B.

1 Introduction

The boron isotopic composition (δ^{11}B) of benthic foraminifera has been used to reconstruct deep-water pH (Hönisch et al., 2008; Rae et al., 2011; Raitzsch et al., 2020; Yu et al., 2010) and to estimate the Cenozoic evolution of seawater δ^{11}B (Raitzsch and Hönisch, 2013). The underlying mechanism behind the boron isotope method lies in the constant equilibrium fractionation of 27.2 ± 0.6 ‰ between the pH-dependent speciation of trigonal boric acid and the tetrahedral borate in seawater (Klochko et al., 2006), where only the borate ion is incorporated into the foraminifera test (Branson et al., 2015; Hemming and Hanson, 1992).

However, while the number of studies on planktonic foraminiferal δ^{11}B to estimate surface-ocean pH has rapidly increased within the last decade, deep-sea pH reconstructions based on benthic foraminifera are relatively rare (Hönisch et al., 2008; Rae et al., 2011; Raitzsch et al., 2020; Yu et al., 2010). Possible reasons for this might be the lower abundance of benthic foraminifera, compared to planktonic species, and a limited selection of species that truly record bottom-water, rather than pore-water conditions (Rae et al., 2011). Fortunately, there are two suitable candidates, *Cibicidoides wuellerstorfi* and *Cibicidoides mundulus*, that cover a relatively large oceanographic and stratigraphic range, and which have a high boron content of ~12-27 ppm (Raitzsch et al., 2011; Yu and Elderfield, 2007). Although their high [B] may partly compensate for the low abundance in the sediments, in many cases the availability of enough specimens for δ^{11}B analysis remains limiting.

Here, microanalytical techniques such as laser ablation multicollector inductively coupled plasma mass spectrometry (LA-MC-ICPMS) and secondary ion mass spectrometry (SIMS) can help to overcome the problem of sample limitation. These techniques have already been successfully used for a variety of biogenic carbonates to gain information on biomineralization processes or seasonal pH variations (e.g., Blamart et al, 2007; Fietzke et al, 2015; Howes et al., 2017; Kaczmarek et al., 2015a; Mayk et al., 2020; Rollion-Bard and Erez, 2010; Sadekov et al., 2019). On the other hand, microanalytical analysis of δ^{11}B is usually afflicted with larger uncertainties in terms of repeatability and reproducibility, as well as of natural δ^{11}B heterogeneity within single shells and within a population. In addition, some recent studies using LA-MC-ICPMS suggest correction modes for measured δ^{11}B values because detected interferences on the ^{10}B peak, possibly due to scattered Ca ions from the carbonate sample, can result in large offsets from the expected value (Thil et al, 2016; Sadekov et al., 2019; Standish et al., 2019), whereas in other studies this matrix-induced effect was not observed (Fietzke et al., 2010; Kaczmarek et al., 2015b; Mayk et al., 2020).

Also, the reported analytical reproducibility for δ^{11}B in biogenic carbonate using LA-MC-ICPMS differs considerably among different studies, ranging between ±0.22 and 1.60 ‰ (2σ=2 standard deviations), determined from repeated measurements of either a carbonate or glass standard (Fietzke et al., 2010; Kaczmarek et al., 2015b; Mayk et al., 2020; Sadekov et al., 2019; Standish et al., 2019; Thil et al., 2016). As there is no standardized protocol nor a commercially available homogenized δ^{11}B carbonate standard for determining the analytical uncertainty of LA-MC-ICPMS, this issue remains the most challenging task to compare the different labs and instruments. The most commonly used carbonate standards with well-constrained boron isotopic compositions are samples from a coral (JCp-1) and a giant clam (JCt-1),

provided by the *Geological Survey of Japan* (e.g., Inoue et al., 2004; Okai et al., 2004). However, for microanalytical analysis the standard is usually powdered in a mortar and finally pressed to a pellet, which is produced individually in each laboratory, thus potentially resulting in different heterogeneities (e.g., through different grain sizes or applied pressures) in each pellet. This issue is also true for SIMS analyses, and the reported reproducibility is strongly linked to the in-house reference material used (e.g., Kaseman et al., 2009; Rollion-Bard and Blamart, 2014).

In this study, we investigate a population of 23 specimens of *C. wuellerstorfi*, which is a widely used benthic foraminifer species in paleoceanographic studies, to extend our knowledge of $\delta^{11}B$ variability within and between individuals. The aim of our study is to demonstrate the capabilities and limitations of $\delta^{11}B$ analyses in *C. wuellerstorfi* on a microscale. For this purpose, we used the femtosecond LA-MC-ICPMS and SIMS techniques and compared the results with bulk-solution MC-ICPMS. Finally, we examine the size of population required for targeted $\delta^{11}B$ uncertainty levels in paleoceanographic studies using LA-MC-ICPMS.

2 Material and Methods

2.1 Foraminifer samples

For this study, we used sediment samples from GeoB core 1032-3, taken in the Angola Basin on the Walvis Ridge at a water depth of 2505 m. From a Holocene interval (6-8 cm, 5.6 ka), 23 pristine (glassy) shells of the benthic foraminifer species *C. wuellerstorfi* from the size fraction >350 µm were picked and prepared for subsequent microanalytical analysis. Five large specimens (>400 µm) were embedded in epoxy and polished down to a planar surface for SIMS analyses, while the remaining 18 specimens were mounted on carbon tape for LA measurements. From these 18 individuals, two large tests were analyzed for detailed chamber-to-chamber variability, while the remaining 16 tests were used to measure quasi-bulk $\delta^{11}B$ by ablating large shell areas, preceded by measurements of the smaller umbilical knob area.

2.2 Secondary ion mass spectrometry

For the ion microprobe analyses, we used the same technique as described in Rollion-Bard et al. (2003) and Blamart et al. (2007). Boron isotopic compositions were measured with the Cameca ims 1270 ion microprobe at CRPG-CNRS, Nancy, France. A primary beam of $^{16}O^-$ ions generated using a Radio Frequency Plasma source (Malherbe et al, 2016) with an intensity of 50 nA was focused to a spot of about 20 µm. A mass resolution of 3000 was used for B isotope analyses, allowing the elimination of all isobaric interferences. Boron isotopes were analyzed in mono-collection mode using the central electron multiplier. The dead time of the electron multiplier was determined before the analytical session and set to 65 ns. A pre-sputtering of 120 s was applied before the analysis itself. The typical intensities of $^{11}B^+$ in foraminifer tests were between 2000 and 4500 counts per second (cps), depending on the boron concentration. The analysis consists of 60 cycles of 10 s for $^{10}B^+$ and 6 s for $^{11}B^+$, respectively. The reference material was a calcium carbonate with a B concentration of 22 ppm

and a $\delta^{11}B$ of 16.76 ± 0.11 ‰, relative to the standard reference material (SRM) NIST 951 (WP22, value determined at IPGP using the method of Louvat et al, 2014). The reproducibility, as estimated by multiple measurements of the reference material, was 2.48 ‰ (2σ, n=8), and is very close to the predicted 2σ uncertainty derived from counting statistics.

2.3 Femtosecond laser ablation MC-ICPMS

Boron isotope measurements were performed using a customized UV-femtosecond laser ablation system coupled to a Plasma II MC-ICPMS (Nu Instruments) at the AWI, Bremerhaven. The laser ablation system is based on a Ti-sapphire regenerative amplifier system (Solstice, Spectra-Physics, USA) operating at the fundamental wavelength of 775 nm with a pulse width of 100 fs and pulse energy of 3.5 mJ/pulse. Consecutive frequency conversion results in an output beam with a wavelength in the UV spectra (193 nm) and a pulse energy of 0.08 mJ. The short femtosecond pulses were shown to have major advantages over nanosecond pulses for a wide range of element and isotope ratios with respect to laser-induced and particle-size-related fractionation, thus enabling non-matrix-matched calibrations (e.g., Horn and von Blanckenburg, 2007; Steinhoefel et al., 2009).

The sample and standard materials were mounted in an ablation chamber with an active volume of ca. 45 cm^3 and ablated in a helix-mode scan at a speed of 2 mm s^{-1} by using a laser spot size of ~40 μm. This technique allows producing ablation craters of almost any diameter, in this study ranging from ~80 μm for analysis of single-chamber to ~400 μm to cover whole shells. The aerosol was transported via a He gas flow (~0.5 L/min) and admixed with Ar gas (~0.5 L/min) before entering the MC-ICP-MS. Torch position, ion optics and gas flows were optimized to gain maximum signal intensity and stability on ^{10}B and ^{11}B peaks. The mass spectrometer was equipped with standard Ni sample and skimmer cones for dry plasma conditions. The radio frequency power was set to 1300 W. Boron isotopes were determined on Daly detectors, where high-mass D5 was used for ^{11}B and D0 for ^{10}B. Each measured sample $^{11}B/^{10}B$ was normalized to $^{11}B/^{10}B$ measurements of the glass standard NIST SRM 610 ($\delta^{11}B$=0 ‰ NBS 951), using the Standard-Sample-Bracketing technique. The analyses were performed at low mass resolution (M/ΔM ~2000, 5‰), which was sufficient to resolve all interferences.

We performed mass scans on the peaks of ^{10}B and ^{11}B for both gas blanks (laser off) and measurements on carbonate (laser on) (Fig. 1) to investigate possible effects by scattered ions of matrix elements as observed in some recent studies (Sadekov et al., 2019; Standish et al., 2019). For our set-up, we can exclude such matrix-induced effects, which is in line with Fietzke et al. (2010) and Mayk et al. (2020). Hence, there was no need to correct the raw LA data as done in the recent studies by Sadekov et al. (2019) and Standish et al. (2019). Before analysis, sample and standard materials were pre-ablated to remove potential surface contamination. Laser repetition rates ranged between 12 and 60 Hz to match the signal intensity between carbonate samples and standard material NIST SRM 610 (~300,000 cps on ^{11}B). As ablation efficiency and hence signal intensity may vary with progressively increasing surface roughness and crater depth, we adjusted the repetition rate, if required, to target intensity matching between sample and standard. Whereas this approach could result in bulgy time-resolved isotope signals, as shown in Fig. 2, clean calcium carbonate was identified from a plateau-like $^{11}B/^{10}B$ signal.

125 Conversely, any contaminated phase from partial ablation of clay infillings, indicated by dropping $^{11}B/^{10}B$ ratios accompanied by rising [B], were excluded from further data treatment (Fig. 2).

Each analysis was preceded by an on-peak gas blank measurement of 60 s on ^{10}B and ^{11}B, which was subtracted from the LA signal. The LA analysis itself was assessed by calculating the mean of the blank-corrected $^{11}B/^{10}B$ signal within an interval of up to 370 cycles (1 s each), where all data exceeding two standard deviations were removed as outliers. After analysis, B was

130 washed out for 120 to 180 s until reaching background levels before a new measurement was started. A typical blank had ~7,000 cps on ^{11}B at the beginning of a session, but decreased to less than 3,000 cps during the course of a day. As signal intensity on ^{11}B was aimed at ~300,000 cps, the signal-to-noise ratio was in the order of ~100.

Accuracy of boron isotope measurements was frequently checked by ablating an in-house carbonate standard that was also used for SIMS analysis (i.e. WP22, Rollion-Bard et al, 2003). The average $\delta^{11}B$ of 16.49 ± 1.26 ‰ (2σ, n=20) for WP22 is

135 very close to the bulk solution values ($\delta^{11}B$=16.60 ± 0.30 ‰ (2σ, n=6) measured at AWI, and $\delta^{11}B$=16.76 ± 0.11 ‰ measured at IPGP). As the measurement uncertainty is mainly dependent on the ablation time, we report measurement uncertainties (as 2σ) for each $\delta^{11}B$ analysis as a function of analysis time, which was determined from multiple measurements of NIST glass standards and carbonate standards, and which is very close to the predicted uncertainty based on counting statistics (Fig. 3).

140 **2.4 Bulk solution MC-ICPMS**

After LA analyses, the 18 shells were carefully removed from the carbon tape and cleaned following the procedure outlined by Raitzsch et al. (2018). Briefly, foraminifer shells were gently crushed under a binocular between two glass slides and transferred to Eppendorf vials. After the clay removal and oxidative cleaning steps, the samples were leached in 0.001 N HNO_3, and finally dissolved in 60 μL of 1 N HNO_3.

145 Prior to boron isotope analysis, we used the micro-distillation technique to separate B from the calcium carbonate matrix (Gaillardet et al., 2001; Misra et al., 2014; Raitzsch et al., 2018; Wang et al., 2010). The distillate was diluted with 400 μL of 0.3 N HNO_3. The B concentration of a small aliquot was determined using a quick (20 s) on-peak measurement of ^{11}B on Faraday cup H9 using a Nu Plasma II MC-ICPMS (AWI, Bremerhaven). The remainder of the sample was then diluted to yield a solution with a [B] of 3 ppb and concentration-matched with the SRM NBS 951 to within ±3 %.

150 For isotope ratio measurements, boron was collected on Daly detectors, where high-mass D5 was used for ^{11}B and D0 for ^{10}B. Boron isotope data were measured in triplicate using the standard-sample-bracketing technique and reported in delta notation normalized to SRM NBS 951:

$$\delta^{11}B_{sample} = \left(\frac{^{11}B/^{10}B_{sample}}{^{11}B/^{10}B_{NIST\,951}} - 1 \right) * 1000 \qquad (1)$$

When 2σ of the mean derived from the triplicate was smaller than the long-term reproducibility (0.30 ‰), we report the

155 latter as the measurement uncertainty. In addition, a small fragment of an in-house carbonate reference material WP22, used

for our SIMS and LA-MC-ICPMS study, was cleaned and measured exactly the same way as the foraminifera sample to obtain a bulk $\delta^{11}B$ value for comparison (16.60 ± 0.30 ‰). This value is almost identical to that measured at IPGP using the bulk solution ICP-MS (16.76 ± 0.11 ‰).

3 Results and discussion

3.1 Intra-shell $\delta^{11}B$ variability

The results from SIMS measurements conducted on 5 large specimens reveal a high $\delta^{11}B$ variability ranging between 4.6 and 6.8 (mean 5.2) ‰ (2σ, 2 standard deviations of n individual measurements) within single shells, based on 8 to 19 single spot analyses on each shell. A similar variability of 4.4 ‰ (2σ) on average is observed for measurements within single chambers (Fig. 4). Since it is difficult to distinguish between the very small (i.e. the juvenile) chambers in the central part, we allocated these measurements to the umbilical "knob", which is also equivalent to the thick central part of the spiral side used for LA measurements. If $\delta^{11}B$ is averaged for each chamber (1 to 3 analyses per chamber), the mean variability between chambers is 4.2 ‰ (2σ) (Fig. 4). The two specimens measured chamber by chamber with LA also show variable $\delta^{11}B$, but with a much lower variation of ~1.1 ‰ (2σ), compared to the SIMS data (Fig. 4). The average $\delta^{11}B$ variability from all 16 shells measured multiple times is ~1.3 ‰ (2σ).

Here the question arises whether the difference in $\delta^{11}B$ variability between the two methods is due to differences in analytical uncertainty or different scales of natural heterogeneity. If we consider an average uncertainty of ±0.9 ‰ for LA (Fig. 3), intra-shell variability is reduced from 1.3 ‰ to 0.4 ‰. As the 2σ measurement uncertainty for SIMS is roughly ±2.5 ‰, the remaining difference in variability between SIMS and LA methods of ~2.3 ‰ is likely due to the different sampling volumes, and hence related to heterogeneous boron isotopic distribution in the test. While the spot size for the SIMS method is ~20 µm and ~1 µm in depth, the laser-ablated volume ranges from 80 to 100 µm in diameter (Fig. 4) and approximately 10 µm in depth. Consequently, the ~200 times larger volume analyzed by LA would reduce the $\delta^{11}B$ variability detected by SIMS to ~0.2 (=2.3/$\sqrt{200}$) ‰. Hence we argue that the "true" $\delta^{11}B$ heterogeneity is scale-dependent and assumedly in the order of ~3 and ~0.4 ‰ (2σ) on a ~20 and 100 µm grid, respectively.

To examine potential systematic trends in $\delta^{11}B$ among successive chambers, we calculated the residual boron isotopic composition $\Delta\delta^{11}B$ for each site within each shell by comparing the B isotopic composition of a single chamber $\delta^{11}B_{single}$ with the mean value of the shell $\delta^{11}B_{mean}$:

$$\Delta\delta^{11}B = \delta^{11}B_{single} - \delta^{11}B_{mean} \qquad (2)$$

The SIMS data suggest that $\Delta\delta^{11}B$ tends to decrease from the penultimate chamber (f-1) towards chamber f-5 by roughly 4 ‰ (Fig. 4), whereas no systematic change exists between chambers f-6 and the juvenile chambers. However, it is compelling that also the LA results suggest a decreasing trend in $\Delta\delta^{11}B$ from the final chambers towards chamber f-5 by more than 0.5 ‰, while in the earlier chambers no systematic change can be observed (Fig. 4). For both methods, Wilcoxon-Mann-

Whitney tests and Welch's t-tests suggest that the $\Delta\delta^{11}B$ change between the final chambers and f-5 is statistically insignificant at a 95 % significance level (p-values ≥ 0.07). However, decreasing $\delta^{11}B$ from the final chamber towards earlier chambers would be in line with the LA study by Sadekov et al. (2019) showing a ~2 ‰ decrease along the last whorl of *C.*
190 *wuellerstorfi*. A similar pattern was also observed for B/Ca, with the highest value in the final chamber (Raitzsch et al., 2011; Sadekov et al., 2019), suggesting a strong biological influence or kinetic (i.e. growth rate) effect on boron incorporation. An in-depth discussion of biological/calcification processes is beyond the scope of this study, but the discovery of such high variability has implications for the use of $\delta^{11}B$-microanalytical techniques in paleoceanographic studies (e.g., Rollion-Bard and Erez, 2010).

195 Another notable feature derived from LA and SIMS is the elevated $\delta^{11}B$ (by ~0.5 ‰ on av.) of the umbilical knob, compared to the whole-shell $\delta^{11}B$. This is confirmed by supplementary ablation of the knob of individuals, which were used for whole-shell analysis in section 3.2. On average, umbilical knob $\delta^{11}B$ was ~0.4 ‰ higher than the value derived from the larger ablated area (see inset picture in Fig. 7), although this behavior is not systematic and was observed in only two thirds of the cases.

200 **3.2 Inter-shell $\delta^{11}B$ variability**

Apart from the seven specimens used for inspecting the chamber-to-chamber variability, 16 individuals of *C. wuellerstorfi* were laser-ablated using a large area of at least 300 μm in diameter to cover a major part of the spiral side, and in 14 specimens subsequently analyzed for the composition of the thicker umbilical knob using a smaller crater (inset picture in Fig. 7). This way, we approached quasi-bulk $\delta^{11}B$ values for single shells. Together with the $\delta^{11}B$ medians from the two
205 specimens described in the previous section, a total of 18 shells were used for determining the inter-shell $\delta^{11}B$ variability using LA-MC-ICPMS (Fig. 5). It should be noted that we usually report the average as median, since it is less sensitive to outliers than the mean, and also reflects the average of a non-uniform distribution. For SIMS analyses, the medians of single-spot analyses were calculated for each of the 5 shells.

The SIMS data reveal a huge spread of single-spot $\delta^{11}B$ across the 5 specimens (section 3.1), but the $\delta^{11}B$ values averaged for
210 each shell exhibit a narrower range between tests, with a median $\delta^{11}B$ of 16.08 ± 2.70 ‰ (2σ) (Fig. 5). In contrast, the single-site LA data across all 18 individuals show a smaller variation in $\delta^{11}B$ than the SIMS data, where the values averaged for each shell yield a median of 15.90 ± 1.62 ‰ (2σ). Both the average $\delta^{11}B$ measurement uncertainty for LA of ±0.9 ‰ (2σ) and the variation difference between foraminiferal shells and WP22 of ~0.4 ‰ suggest a residual inter-shell variability in the order of 0.4 to 0.7 ‰. Similarly, if an uncertainty of ±2.50 ‰ (2σ) for SIMS measurements is taken into account, the
215 remaining inter-shell variability is only ~0.2 ‰. Therefore, we estimate the "true" variability between shells of a population to be ~0.4 ‰, which is the same as the variation estimated for the intra-shell variability (section 3.1).

For shells where both large areas and knobs were measured (n=14), it is interesting to note that if only the large LA craters are considered, the mean $\delta^{11}B$ is 15.87 ± 1.78 ‰ (2σ), while it is 16.27 ± 2.75 ‰ (2σ), if solely the small LA craters are taken into account (cf. Fig. 7, inset picture). As the volume of the large LA craters is ~3 times larger than the smaller ones,

220 the resulting variability among means of 3 resampled small-crater values is 1.59 (=2.75/√3) ‰ (2σ), which is quite close to the 1.78 ‰ derived from large craters, and confirms our conclusion that the $\delta^{11}B$ variability is dependent on the scale at which it is measured.

3.3 Bulk solution $\delta^{11}B$

Both the SIMS and LA results reveal median values that match the bulk $\delta^{11}B$ of 15.99 ± 0.30 ‰ (2σ) measured in solution to
225 within analytical uncertainties (Fig. 5). It should be noted again that the same specimens measured in solution had been measured before by LA, ensuring that we compare different techniques based on the same set of samples. Similarly, the average $\delta^{11}B$ of 16.48 ± 1.26 ‰ (2σ) in the reference material WP22 determined with LA-MC-ICPMS is not distinguishable from the bulk solution value of 16.60 ± 0.30 ‰ (2σ), which confirms the robustness of the LA technique, and also the SIMS results, as the median foraminifera values are identical for LA and SIMS techniques.
230 The $\delta^{11}B$ values obtained from all three methods fit in with the calibration data set for *C. wuellerstorfi* from the study by Rae et al. (2011) (Fig. 6), and confirm that the boron isotopic composition in this species closely matches the one of borate of ambient seawater. Further, it proves that LA-MC-ICPMS and SIMS yield accurate results for $\delta^{11}B$, if the data set is large enough to overcome the issues of intra- and inter-shell variability (~0.4 ‰), and analytical uncertainty of micro-analytical techniques (~±0.9 and ±2.5 ‰ for LA and SIMS, respectively).

235 3.4 Implications for paleoreconstruction studies

The large intra- and inter-shell variations in $\delta^{11}B$ described in sections 3.1 and 3.2 raises the question whether microanalytical techniques such as SIMS or LA-MC-ICPMS can be used for analyzing $\delta^{11}B$ in *C. wuellerstorfi* to reconstruct past deep-water pH. The SIMS method requires careful embedding of foraminifer shells in epoxy and polishing down to a planar surface, which precludes further processing for e.g. bulk solution analyses. However, because the size of the beam
240 spot is small (20 μm or less), it is still possible to measure some other elemental and isotopic ratios at the same location on the sample; e.g. the same foraminifera specimens were used to measure $\delta^{18}O$ (Rollion-Bard et al, 2008), $\delta^{11}B$ (Rollion-Bard and Erez, 2010), and δ^7Li (Vigier et al, 2015). SIMS technique is very useful for biomineralization studies (e.g. Rollion-Bard and Erez, 2010), but for paleoreconstruction of deep-sea pH, where high precision is necessary, it may not be the most appropriate technique for routine downcore $\delta^{11}B$ analysis. However, here we will inspect LA-MC-ICPMS as a potential tool
245 for paleo-pH studies.

To attain information on the number of shells required for accurate LA analysis of $\delta^{11}B$ to within a target uncertainty, we applied a Monte Carlo approach to generate two data sets with 10,000 $\delta^{11}B$ data each, within a quoted uncertainty of ±1.68 ‰ and ±2.75 ‰ (2σ) for "large crater" and "knob" measurements, respectively, as given by the original data set (n=16 and n=14, resp.). The average $\delta^{11}B$ values are considered identical between large craters and umbilical knobs, as in the original
250 data they agree to within analytical uncertainty. Then we applied the 'combn()' function of the R package 'utils v3.4.4' (R Core Team, 2018) on each of the simulated data sets. With this function, we can calculate the uncertainty by generating all

possible combinations of n shells taken from the simulated populations. For instance, if we would randomly pick five shells from this sediment sample, the analyzed δ^{11}B would be accurate to within ±0.75 ‰ with a probability of 95 %, if large areas, and ±1.22 ‰, if only the knob areas were analyzed. If we targeted a standard uncertainty of ±0.50 ‰, which is equivalent to a pH uncertainty of roughly ±0.1, we would need to measure ~12 specimens with LA, if large areas, and ~14 specimens, if only the knob areas were analyzed (Fig. 7). The relationship between number of analyzed shells (n) and the estimated 2σ uncertainty is given by the quoted variability u_q, i.e. the measured δ^{11}B variation across a population (as 2σ), and n:

$$2\sigma = \frac{u_q}{\sqrt{n}} \qquad (3)$$

Given that the analysis uncertainty of the same amount measured in solution is about ±0.3 ‰, bulk solution analysis appears to be the more convenient technique for reconstructing paleo-pH. On the other hand, the LA technique may be useful for generating high-resolution records, where sharp pH trends would partly compensate for the larger standard uncertainty or when only few foraminifera specimens are available. Further, LA, like SIMS, has the potential to gain insight into ontogenetic δ^{11}B variations, helping to better understand the biological uptake of boron during chamber formation.

5 Conclusions

Microanalytical methods such as SIMS or LA-MC-ICPMS are potentially powerful tools for studying biomineralization processes or possible alternatives to conventional bulk solution analysis of δ^{11}B in benthic foraminifera, if sample material is limited. For this study, we measured a population of 23 *C. wuellerstorfi* in total using SIMS and femtosecond LA-MC-ICPMS and compared the results with the bulk-solution δ^{11}B, revealing consistent average values among the different techniques. While the medians agree to within ±0.1 ‰, a large intra-shell variability was observed, with up to 6.8 ‰ and 4.5 ‰ (2σ) derived from the SIMS and LA methods, respectively. We propose that the larger spread for SIMS, compared to LA, can be attributed to the much smaller volume (~200⁻¹) of calcite being analyzed in each run, and hence supposedly reflects a larger heterogeneity of δ^{11}B in the foraminiferal test on a smaller scale. When analytical uncertainties and scale-dependent differences in δ^{11}B variations are taken into account, the intra-shell variability is likely in the order of ±0.4 and 3 ‰ (2σ) on a 100 and 20 μm scale, respectively.

The δ^{11}B variability between shells exhibits total ranges of ~3 ‰ for both techniques, suggesting that a number of shells needs to be analyzed for accurate mean δ^{11}B values. We applied a simple resampling method and conclude that about 12 shells of *C. wuellerstorfi* must be analyzed using LA-MC-ICPMS to obtain an accurate average value to within ±0.5 ‰ (2σ). Hence, we suggest that, based on this high number of required individuals, the bulk solution MC-ICPMS method remains the first choice for analysis of δ^{11}B in routine paleo-pH studies.

Data availability

The boron isotope data collected for this study are available from Table S1 in the supplement.

Author contribution

MR, CRB, IH, and JB conceived the study (conceptualization). MR, CRB, and PL carried out measurements, analyzed the data, and performed data statistics (data curation, formal analysis, investigation). AB, KUR, and GS maintained and provided access to analytical instruments at AWI (resources). JB, CRB, and IH raised funding for the French-German project 'B2SeaCarb' (funding acquisition). MR produced the figures for the manuscript (visualization). MR and CRB wrote the first draft of the manuscript (writing – original draft), and all authors interpreted, edited, and reviewed the manuscript (writing – review & editing).

Competing interests

The authors declare that they have no conflict of interest.

Acknowledgements

This research was carried out in the framework of the joint French/German project 'B2SeaCarb' and was supported by the Deutsche Forschungsgemeinschaft (DFG) grant number BI 432/10-1 to JB and DFG grant number HO 3257/5-1 to IH. On the French side, the project was supported by the French National Research Agency (ANR) grant number ANR-16-CE92-0010 to CRB. CRB thanks N. Bouden (CRPG) for his technical help, and the MARUM GeoB core repository is acknowledged for providing sediment samples.

References

Blamart, D., Rollion-Bard, C., Meibom, A., Cuif, J.-P., Juillet-Leclerc, A. and Dauphin, Y.: Correlation of boron isotopic composition with ultrastructure in the deep-sea coral *Lophelia pertusa*: Implications for biomineralization and paleo-pH, Geochem. Geophys. Geosyst., 8(12), Q12001, doi:10.1029/2007GC001686, 2007.

Branson, O., Kaczmarek, K., Redfern, S. A. T., Misra, S., Langer, G., Tyliszczak, T., Bijma, J. and Elderfield, H.: The coordination and distribution of B in foraminiferal calcite, Earth Planet. Sci. Lett., 416, 67–72, doi:10.1016/j.epsl.2015.02.006, 2015.

Fietzke, J., Heinemann, A., Taubner, I., Böhm, F., Erez, J. and Eisenhauer, A.: Boron isotope ratio determination in carbonates via LA-MC-ICP-MS using soda-lime glass standards as reference material, J. Anal. At. Spectrom., 25(12), 1953, doi:10.1039/c0ja00036a, 2010.

Fietzke, J., Ragazzola, F., Halfar, J., Dietze, H., Foster, L. C., Hansteen, T. H., Eisenhauer, A. and Steneck, R. S.: Century-scale trends and seasonality in pH and temperature for shallow zones of the Bering Sea, PNAS, 112(10), 2960–2965, doi:10.1073/pnas.1419216112, 2015.

Gaillardet, J., Lemarchand, D., Göpel, C. and Manhès, G.: Evaporation and Sublimation of Boric Acid: Application for Boron Purification from Organic Rich Solutions, Geostand. Newsl., 25(1), 67–75, doi:10.1111/j.1751-908X.2001.tb00788.x, 2001.

Hemming, N. G. and Hanson, G. N.: Boron isotopic composition and concentration in modern marine carbonates, Geochim. Cosmochim. Acta, 56(1), 537–543, doi:10.1016/0016-7037(92)90151-8, 1992.

Hönisch, B., Bickert, T. and Hemming, N. G.: Modern and Pleistocene boron isotope composition of the benthic foraminifer *Cibicidoides wuellerstorfi*, Earth Planet. Sci. Lett., 272(1–2), 309–318, doi:10.1016/j.epsl.2008.04.047, 2008.

Horn, I. and von Blanckenburg, F.: Investigation on elemental and isotopic fractionation during 196 nm femtosecond laser ablation multiple collector inductively coupled plasma mass spectrometry, Spectrochim. Acta Part B At. Spectrosc., 62(4), 410–422, doi:10.1016/j.sab.2007.03.034, 2007.

Howes, E. L., Kaczmarek, K., Raitzsch, M., Mewes, A., Bijma, N., Horn, I., Misra, S., Gattuso, J.-P. and Bijma, J.: Decoupled carbonate chemistry controls on the incorporation of boron into *Orbulina universa*, Biogeosciences, 14(2), 415–430, doi:https://doi.org/10.5194/bg-14-415-2017, 2017.

Inoue, M., Nohara, M., Okai, T., Suzuki, A. and Kawahata, H.: Concentrations of Trace Elements in Carbonate Reference Materials Coral JCp-1 and Giant Clam JCt-1 by Inductively Plasma-Mass Spectrometry, Geostand. Geoanalytical Res., 28(3), 411–416, 2004.

Kaczmarek, K., Horn, I., Nehrke, G. and Bijma, J.: Simultaneous determination of δ^{11}B and B/Ca ratio in marine biogenic carbonates at nanogram level, Chem. Geol., 392, 32–42, doi:10.1016/j.chemgeo.2014.11.011, 2015a.

Kaczmarek, K., Langer, G., Nehrke, G., Horn, I., Misra, S., Janse, M. and Bijma, J.: Boron incorporation in the foraminifer *Amphistegina lessonii* under a decoupled carbonate chemistry, Biogeosciences, 12(6), 1753–1763, doi:10.5194/bg-12-1753-2015, 2015b.

Kasemann, S. A., Schmidt, D. N., Bijma, J. and Foster, G. L.: In situ boron isotope analysis in marine carbonates and its application for foraminifera and palaeo-pH, Chem. Geol., 260(1–2), 138–147, doi:10.1016/j.chemgeo.2008.12.015, 2009.

Klochko, K., Kaufman, A. J., Yao, W., Byrne, R. H. and Tossell, J. A.: Experimental measurement of boron isotope fractionation in seawater, Earth Planet. Sci. Lett., 248, 276–285, doi:10.1016/j.epsl.2006.05.034, 2006.

Louvat, P., Moureau, J., Paris, G., Bouchez, J., Noireaux, J. and Gaillardet, J.: A fully automated direct injection nebulizer (d-DIHEN) for MC-ICP-MS isotope analysis: application to boron isotope ratio measurements, J. Anal. At. Spectrom., 29(9), 1698–1707, doi:10.1039/C4JA00098F, 2014.

Malherbe, J., Penen, F., Isaure, M.-P., Frank, J., Hause, G., Dobritzsch, D., Gontier, E., Horréard, F., Hillion, F. and Schaumlöffel, D.: A New Radio Frequency Plasma Oxygen Primary Ion Source on Nano Secondary Ion Mass Spectrometry for Improved Lateral Resolution and Detection of Electropositive Elements at Single Cell Level, Anal. Chem., 88(14), 7130–7136, doi:10.1021/acs.analchem.6b01153, 2016.

Mayk, D., Fietzke, J., Anagnostou, E. and Paytan, A.: LA-MC-ICP-MS study of boron isotopes in individual planktonic foraminifera: A novel approach to obtain seasonal variability patterns, Chem. Geol., 531, 119351, doi:10.1016/j.chemgeo.2019.119351, 2020.

Misra, S., Owen, R., Kerr, J., Greaves, M. and Elderfield, H.: Determination of $\delta^{11}B$ by HR-ICP-MS from mass limited samples: Application to natural carbonates and water samples, Geochim. Cosmochim. Acta, 140, 531–552, doi:10.1016/j.gca.2014.05.047, 2014.

Okai, T., Suzuki, A., Terashima, S., Inoue, M., Nohara, M., Kawahata, H. and Imai, N.: Collaborative Analysis of GSJ/AIST Geochemical Reference Materials JCp-1 (Coral) and JCt-1 (Giant Clam), Chikyu Kagaku, 38(4), 281–286, 2004.

R Core Team: A Language and Environment for Statistical Computing, R Foundation for Statistical Computing, Vienna. [online] Available from: https://www.R-project.org, 2018.

Rae, J. W. B., Foster, G. L., Schmidt, D. N. and Elliott, T.: Boron isotopes and B/Ca in benthic foraminifera: Proxies for the deep ocean carbonate system, Earth Planet. Sci. Lett., 302(3–4), 403–413, doi:10.1016/j.epsl.2010.12.034, 2011.

Raitzsch, M. and Hönisch, B.: Cenozoic boron isotope variations in benthic foraminifers, Geology, 41(5), 591–594, doi:https://doi.org/10.1130/G34031.1, 2013.

Raitzsch, M., Bijma, J., Bickert, T., Schulz, M., Holbourn, A. and Kučera, M.: Eccentricity-paced atmospheric carbon-dioxide variations across the middle Miocene climate transition, Clim. Past Discuss., https://doi.org/10.5194/cp-2020-96, 2020.

Raitzsch, M., Hathorne, E. C., Kuhnert, H., Groeneveld, J. and Bickert, T.: Modern and late Pleistocene B/Ca ratios of the benthic foraminifer *Planulina wuellerstorfi* determined with laser ablation ICP-MS, Geology, 39(11), 1039–1042, doi:https://doi.org/10.1130/G32009.1, 2011.

Raitzsch, M., Bijma, J., Benthien, A., Richter, K.-U., Steinhoefel, G. and Kučera, M.: Boron isotope-based seasonal paleo-pH reconstruction for the Southeast Atlantic – A multispecies approach using habitat preference of planktonic foraminifera, Earth Planet. Sci. Lett., 487, 138–150, doi:https://doi.org/10.1016/j.epsl.2018.02.002, 2018.

Rollion-Bard, C. and Blamart, D.: in Biomineralization Sourcebook: Characterization of Biominerals and Biomimetic Materials, pp. 249–261, CRC Press, Taylor & Francis Group, Boca Raton, FL., 2014.

Rollion-Bard, C. and Erez, J.: Intra-shell boron isotope ratios in the symbiont-bearing benthic foraminiferan *Amphistegina lobifera*: Implications for $\delta^{11}B$ vital effects and paleo-pH reconstructions, Geochim. Cosmochim. Acta, 74(5), 1530–1536, doi:10.1016/j.gca.2009.11.017, 2010.

Rollion-Bard, C., Chaussidon, M. and France-Lanord, C.: pH control on oxygen isotopic composition of symbiotic corals, Earth Planet. Sci. Lett., 215(1), 275–288, doi:10.1016/S0012-821X(03)00391-1, 2003.

Sadekov, A., Lloyd, N. S., Misra, S., Trotter, J., D'Olivo, J. and McCulloch, M.: Accurate and precise microscale measurements of boron isotope ratios in calcium carbonates using laser ablation multicollector-ICPMS, J. Anal. At. Spectrom., 34(3), 550–560, doi:10.1039/C8JA00444G, 2019.

Standish, C. D., Chalk, T. B., Babila, T. L., Milton, J. A., Palmer, M. R. and Foster, G. L.: The effect of matrix interferences on in situ boron isotope analysis by laser ablation multi-collector inductively coupled plasma mass spectrometry, Rapid Commun. Mass Spectrom., 33(10), 959–968, doi:10.1002/rcm.8432, 2019.

Steinhoefel, G., Horn, I. and von Blanckenburg, F.: Matrix-independent Fe isotope ratio determination in silicates using UV femtosecond laser ablation, Chem. Geol., 268(1), 67–73, doi:10.1016/j.chemgeo.2009.07.010, 2009.

Thil, F., Blamart, D., Assailly, C., Lazareth, C. E., Leblanc, T., Butsher, J. and Douville, E.: Development of laser ablation multi-collector inductively coupled plasma mass spectrometry for boron isotopic measurement in marine biocarbonates: new improvements and application to a modern *Porites* coral, Rapid Commun. Mass Spectrom., 30(3), 359–371, doi:10.1002/rcm.7448, 2016.

Vigier, N., Rollion-Bard, C., Levenson, Y. and Erez, J.: Lithium isotopes in foraminifera shells as a novel proxy for the ocean dissolved inorganic carbon (DIC), Comptes Rendus Geoscience, 347(1), 43–51, doi:10.1016/j.crte.2014.12.001, 2015.

Wang, B.-S., You, C.-F., Huang, K.-F., Wu, S.-F., Aggarwal, S. K., Chung, C.-H. and Lin, P.-Y.: Direct separation of boron from Na- and Ca-rich matrices by sublimation for stable isotope measurement by MC-ICP-MS, Talanta, 82(4), 1378–1384, doi:10.1016/j.talanta.2010.07.010, 2010.

Yu, J. and Elderfield, H.: Benthic foraminiferal B/Ca ratios reflect deep water carbonate saturation state, Earth Planet. Sci. Lett., 258(1), 73–86, doi:10.1016/j.epsl.2007.03.025, 2007.

Yu, J., Foster, G. L., Elderfield, H., Broecker, W. S. and Clark, E.: An evaluation of benthic foraminiferal B/Ca and $\delta^{11}B$ for deep ocean carbonate ion and pH reconstructions, Earth Planet. Sci. Lett., 293(1–2), 114–120, doi:10.1016/j.epsl.2010.02.029, 2010.
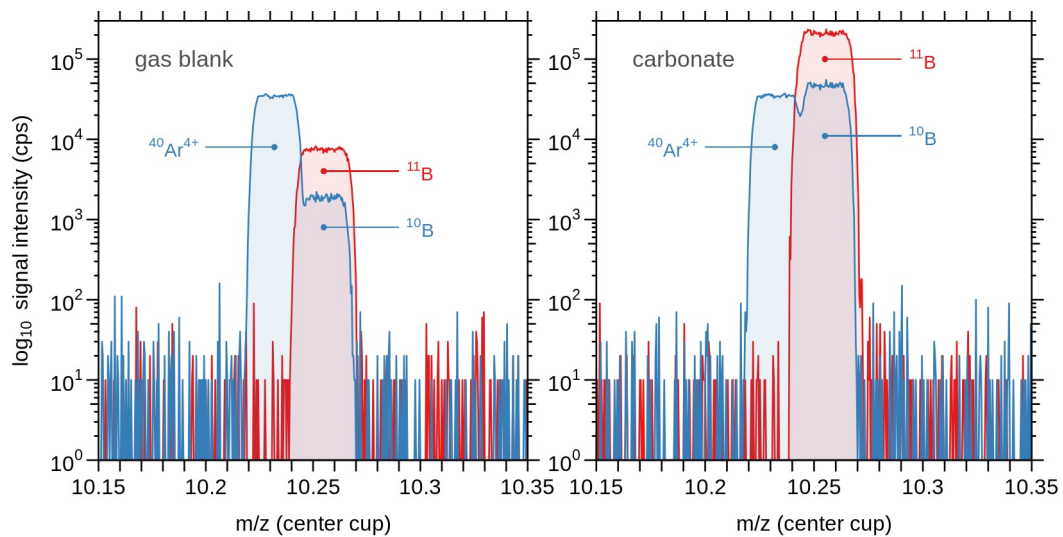
Figure 1: Mass scans over atomic masses 10 (blue) and 11 (red) using Daly detectors, where peak center coincidence appears at ~10.25 amu in the center cup. Left: Gas blank (laser off), showing the typical double peak of $^{40}Ar^{4+}$ and ^{10}B, and the ^{11}B peak. Right: Signal of ablated calcium carbonate (laser on). The baseline exhibits only electronic noise from the Daly detectors, but no sign of unresolved interferences on ^{10}B as matrix-induced scattered Ca ion. Note that the signal intensity is on a logarithmic scale.
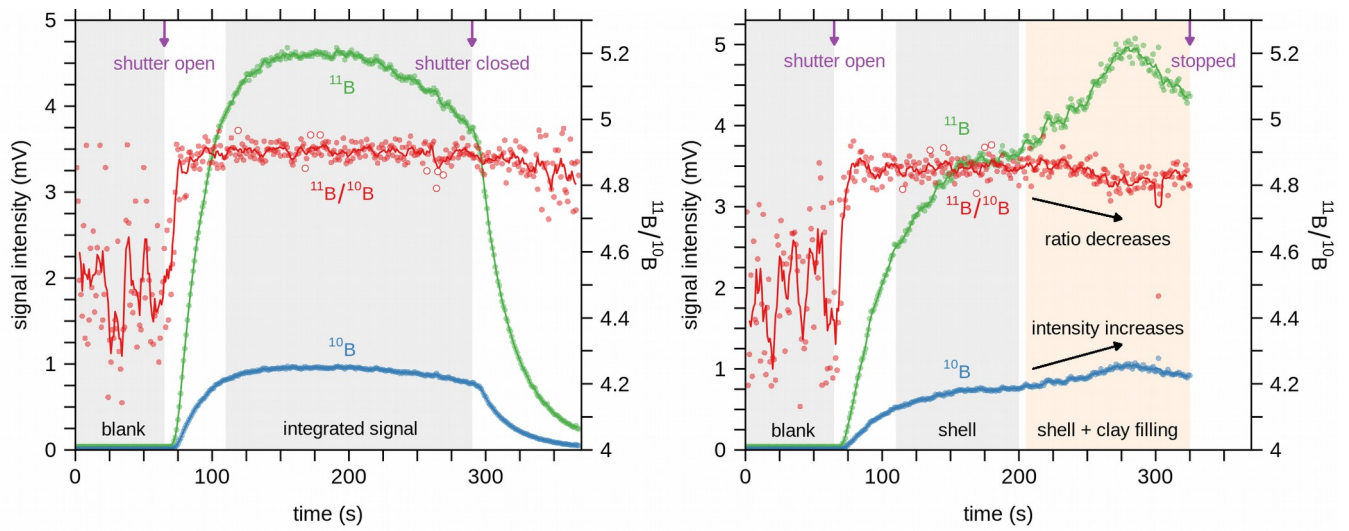
Figure 2: Left: Example of time-resolved laser ablation analysis for ¹⁰B and ¹¹B of a *C. wuellerstorfi* shell using Daly detectors, preceded by a ~60 s blank measurement. Dots represent 1-s cycles, and lines 5-pt running averages. Open symbols are data that are excluded by the 2σ outlier test. Right: Example of a shell that was penetrated by the laser beam, resulting in the ablation of clay infillings.

305
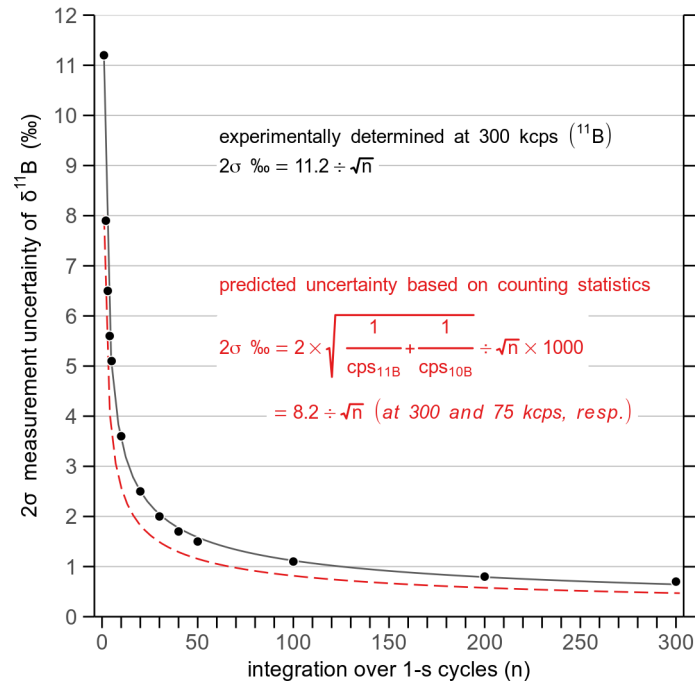
Figure 3: Measurement uncertainty of $^{11}B/^{10}B$ (2σ) at count rates of 300,000 cps (^{11}B) as a function of the laser ablation time. The uncertainty of each boron isotope measurement is calculated based on this relationship (black solid line). A major portion (~70 %) of the measurement uncertainty is related to Poisson-distributed counts (red dashed line).

	SIMS	LA
no of shells analzyed	5	2
interchamber variability (2σ)	±4.2‰	±1.1‰
intrachamber variability (2σ)	±4.4‰	—
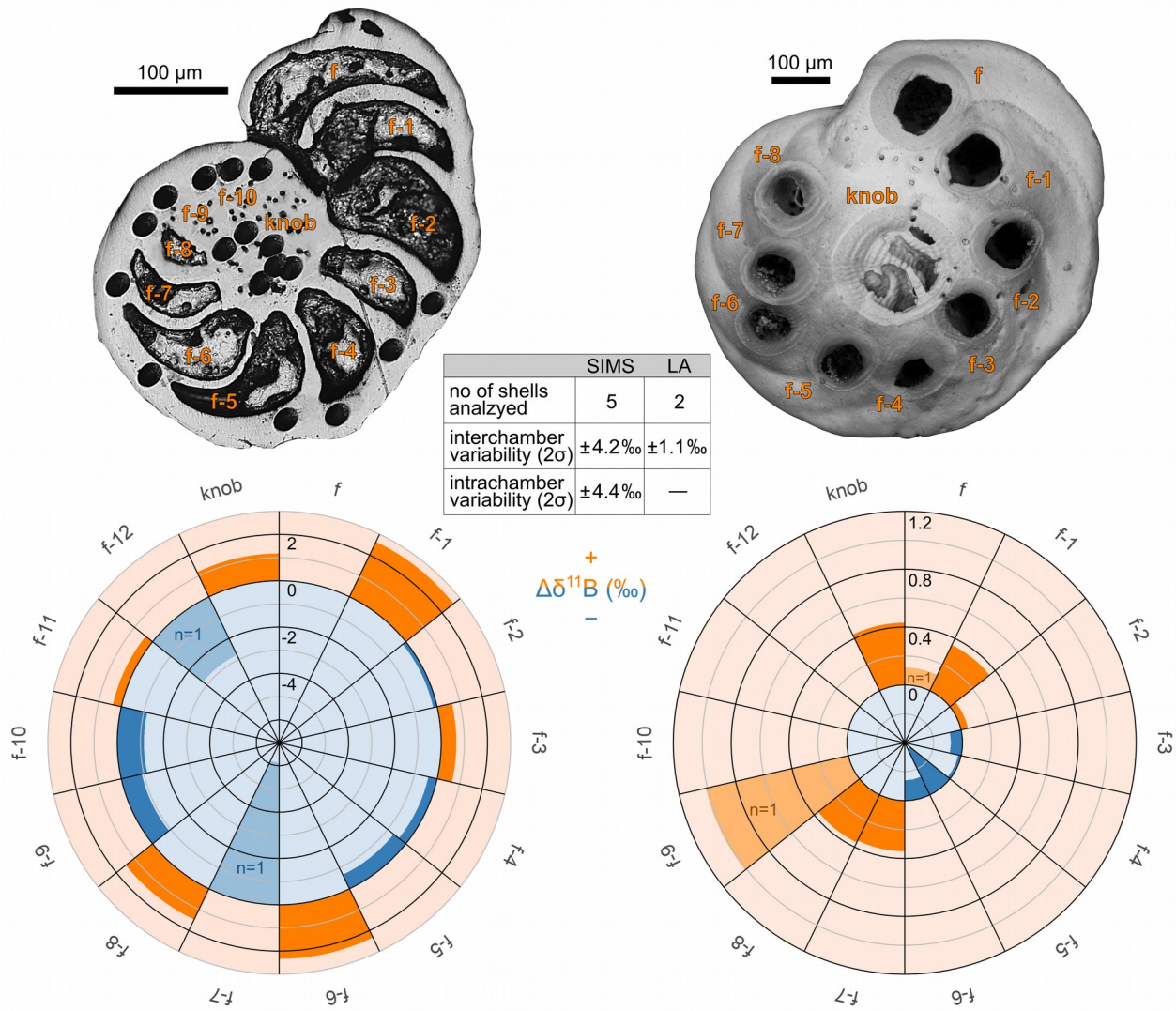
Figure 4: Intra-shell variability of δ^{11}B using SIMS (left panel) and LA-MC-ICPMS (right panel) on selected large individuals of *C. wuellerstorfi*. The residual $\Delta\delta^{11}$B (difference between single spot and mean δ^{11}B, eq. 2) averaged from all analyzed specimens is shown for each chamber (f is the final chamber, f-1 the penultimate one, and so on). Orange color stands for higher-than-mean and blue for lower-than-mean values. Lighter colors indicate data that are based on only one measurement. The inset table summarizes the measured intra-shell variability derived from the two techniques.

310
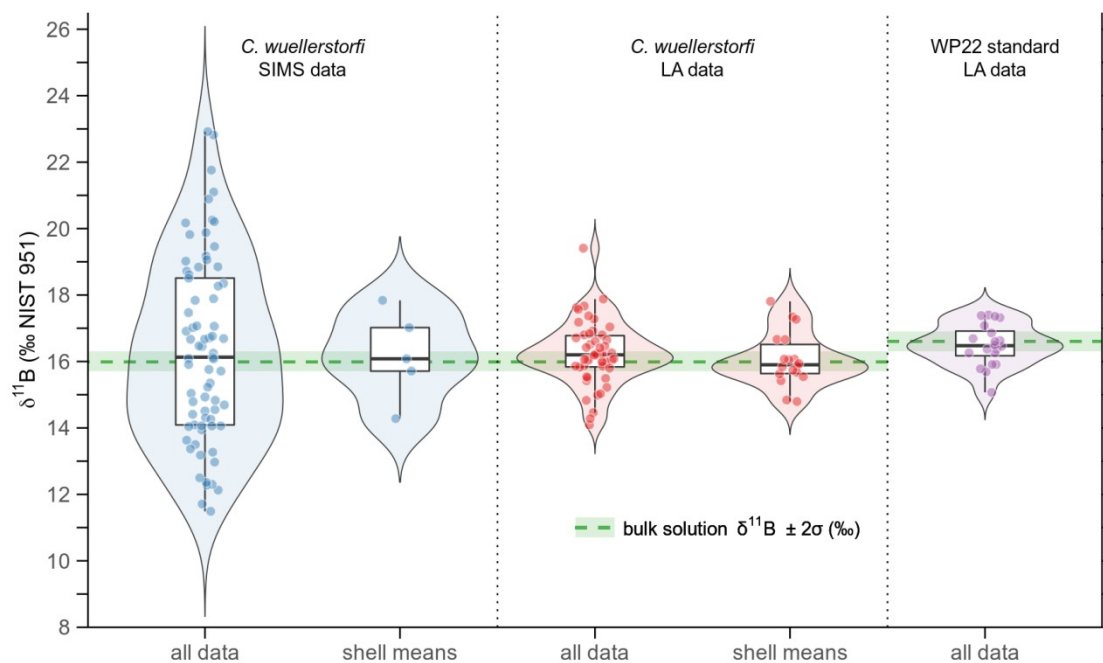
Figure 5: Violin, box and jitter plots showing the distribution of all single-site δ¹¹B values and single-shell means, both for the SIMS and laser ablation techniques. For comparison, the distribution of δ¹¹B values measured on the in-house reference material WP22 is displayed as well. The green dashed lines and bars represent the bulk solution δ¹¹B ± 2σ values.
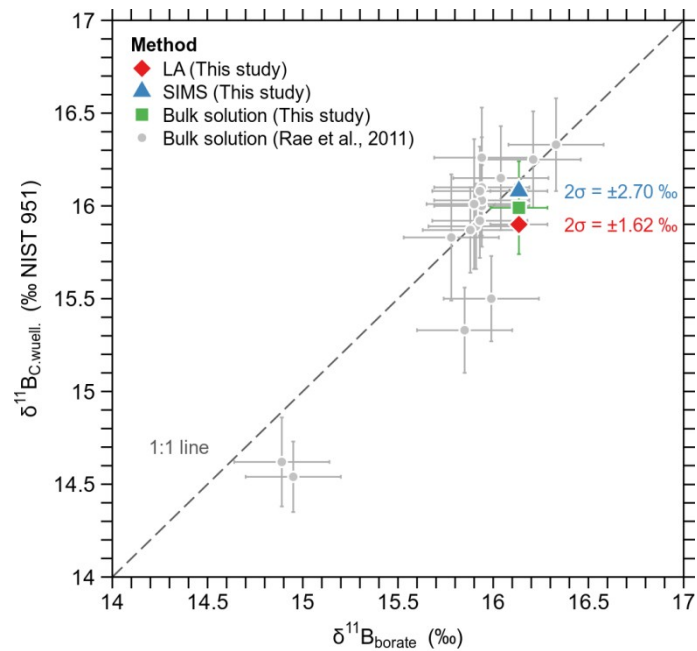
320 **Figure 6: Median δ¹¹B of Holocene (5.6 ka)** *C. wuellerstorfi* **from GeoB core 1032 (Walvis Ridge, South Atlantic) measured with different techniques, shown along with the core-top calibration from (Rae et al., 2011). Note that the bulk solution analysis of this study was carried out on the same population measured before with laser ablation. Pooled δ¹¹B uncertainties for SIMS (n=5 shells) and LA-MC-ICPMS (n=18 shells) are shown as numbers, as error bars exceed the y-axis scale.**

$$2\sigma = u_q/\sqrt{n}$$
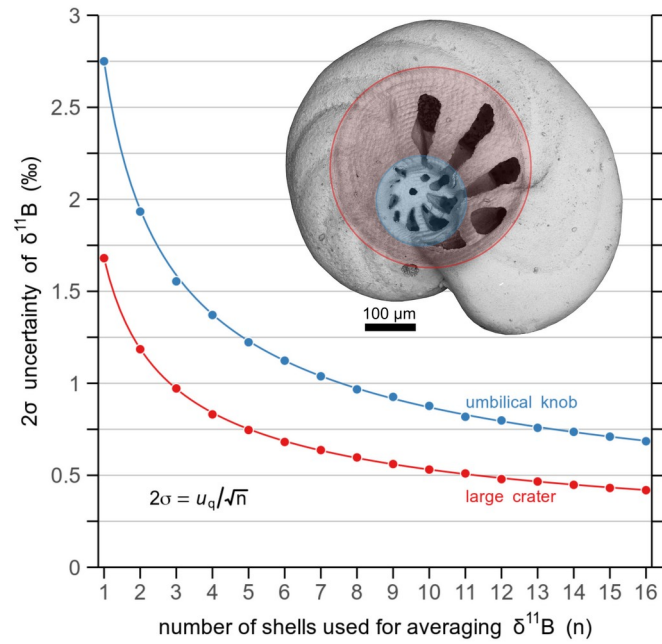
325   **Figure 7: Results from Monte Carlo simulations of 2σ uncertainty for δ¹¹B using LA-MC-ICPMS in relation to the number of analyzed *C. wuellerstorfi* shells (n). In red is the estimated uncertainty based on "large crater", and in blue on "umbilical knob" measurements (cf. inset SEM picture for different areas). The estimated 2σ uncertainty can be described by a function of the quoted uncertainty (u_q) and n (eq. 3).**